

A Compact Electrical Model for Microscale Fuel Cells Capable of Predicting Runtime and I - V Polarization Performance

Min Chen, *Student Member, IEEE*, and Gabriel A. Rincón-Mora, *Senior Member, IEEE*

Abstract—The growing popularity and success of fuel cells (FCs) in aerospace, stationary power, and transportation applications is driving and challenging researchers to complement and in some cases altogether replace the batteries of portable systems in the hopes of increasing functional density, extending runtime, and decreasing size. Direct-methanol fuel cell (DMFC) batteries have now been built and conformed to low-cost technologies and chip-scale dimensions. Conventional FC models, however, fail to accurately capture the electrical nuances and runtime expectancies of these microscale devices, yet predicting that these electrical characteristics are even more critical when designing portable low-power electronics. A Cadence-compatible model of a DMFC battery is therefore developed to capture all pertinent dynamic and steady-state electrical performance parameters, including capacity and its dependence to current and temperature, open-circuit voltage, methanol-crossover current, polarization curve and its dependence to concentration, internal resistance, and time-dependent response under various loading conditions—the model can also be extended to other micro- and macroscale FC technologies. The simulation results of the proposed electrical model are validated and compared against the experimental performance of several DMFC prototypes, resulting in a runtime error of less than 10.8% and a voltage error under various current loads of less than 80 mV for up to 95% of its operational life. The root cause of the remaining errors and relevant temperature effects in the proposed model are also discussed.

Index Terms—Battery, direct-methanol fuel cell (DMFC), electrical model, I - V performance, methanol crossover effects, predicting runtime, temperature drift, transient response.

I. INTRODUCTION

THE HIGH energy densities exhibited by fuel cell (FC) technologies in aerospace, stationary power, and transportation applications [1], [2] have inspired researchers to develop similar solutions for portable and handheld electronics (e.g., cellular phones, personal digital assistants, etc.) [3]–[5], including system-in-package (SiP) modules (e.g., wireless microsensors for *ad hoc* networks) [6]–[10]. The idea is to achieve higher overall energy and power densities than state-of-the-art battery technologies (i.e., nickel metal hydride—NiMH, lithium ion—Li-ion, and others), reducing in the process the overall physical dimensions of microsystems to unprecedented levels.

Manuscript received May 11, 2006; revised September 30, 2006. Paper no. TEC-00148-2006

The authors are with Georgia Tech Analog and Power IC Design Laboratory, School of Electrical and Computer Engineering, Georgia Institute of Technology, Atlanta, GA 30332 USA (e-mail: minchen@ece.gatech.edu; rincón-mora@ece.gatech.edu).

Color versions of one or more of the figures in this paper are available online at <http://ieeexplore.ieee.org>.

Digital Object Identifier 10.1109/TEC.2008.926038

In theory, the energy density of direct-methanol fuel cells (DMFCs) is five times higher than that of Li-ion batteries [3]–[5], which explains why scaling DMFCs to microscale proportions is the subject of research for a growing number of researchers [6]–[10]. Other FC technologies require bulky fuel reformers, heaters, humidifiers, and other mechanical components [11], [12] that are next to impossible to scale down to chip size. In DMFCs, on the other hand, whose operating range includes ambient temperature, the fuel reservoir is directly applied to the membrane and air is used to supply oxygen for its reaction. The end result is a relatively simple solution that is scalable and compatible with low-cost microelectromechanical systems (MEMS) technologies.

To build practical microsystems with volume-, and therefore, energy-limited DMFCs, accurate models predicting current-voltage behavior over time are required. What is more, these models must interface with power-conditioning and application circuits to fully comprehend the electrical performance limits of the overall system. State-of-the-art FC models, however, assume constant fuel-flow and unchanging concentration conditions, and therefore, predict only steady-state, time-independent performance. Microscale DMFCs have limited space to store fuel and must, therefore, account for its use and the resulting changes in concentration. Much like batteries, microscale FCs have finite runtimes.

An electrical model for microscale FCs capable of predicting current and voltage performance over time in a cadence environment, which is an industry standard for designing integrated circuits, is developed and validated in this paper. The presentation is organized as follows. Section II reviews the state of the art in FC models, Section III introduces the proposed model, Section IV discusses the extraction procedure, and Section V validates the model. Discussions on error sources and temperature effects follow in Sections VI and VII, and conclusions in Section VIII.

II. STATE OF THE ART IN FUEL CELL MODELS

DMFCs are electrochemical energy conversion devices that convert methanol and oxygen into carbon dioxide and water, generating electricity in the process. Unlike batteries, DMFCs can produce continuous power supply by assuming that constant fuel-flow conditions exist. As a result, almost all existing FC models only consider time- and concentration-independent characteristics. Generally, however, as load current increases, fuel-limited FCs traverse through three distinct regions of operation: activation, ohmic, and concentration polarization

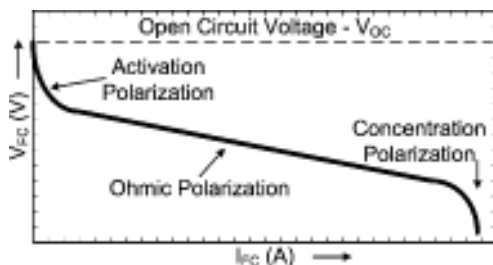


Fig. 1. Polarization curve of a typical fuel cell.

(see Fig. 1). The voltage drop in the activation region, which includes open-circuit and low-current conditions, results from overcoming electronic barriers. The ohmic region, as the name implies, refers to the load-current range for which internal resistance effects are prevalent, that is, to say, when voltage decreases linearly with increasing current. Finally, in the concentration region, there is insufficient fuel flow (i.e., reactant) to supply and sustain high load levels, which results in additional voltage drops.

Most FC models today fall under one of three categories: physically, mathematically, or electrically based. Chemists and physicists, for instance, require models to optimize how FCs are built by describing the physical and chemical character of a given configuration (e.g., thermal gradients, mass transport, electrochemical kinetics, etc.) [13]–[15]. From the perspective of electronic systems, however, these physical models are cumbersome and computationally intensive, especially when considering the complex nature and circuit density of modern electronics.

Mathematical models [16]–[19], like physical models, are not meant to interface with circuits, and consequently, describe the operation of FCs with empirically or semiempirically based equations. The relationship between cell voltages and load currents are tuned with coefficients meant to emulate fuel and air flow and pressure, fuel concentration, temperature, and various other conditions. The resulting model is unable to predict the runtime of a system under various time-varying loads; in other words, it can predict steady-state performance, but not transient response, which is extremely important to electronic engineers.

Electrical models cater to the electronic engineer by describing the electrical behavior of FCs with a combination of voltage sources, resistors, capacitors, inductors, diodes, and transistors. Yu and Yuvarajan [20], for instance, use transistors, inductors, and capacitors readily available in standard SPICE electronic libraries to emulate the steady-state polarization curve response of FCs. To include both steady-state and transient response performance, Famouri and Gemmen [21] employ three dependent voltage sources and a resistor–capacitor network. Garnier *et al.* [22], on the other hand, use a small-signal equivalent circuit derived from electrochemical impedance spectroscopy to describe only static and small-signal transient response.

Although electrical models can be used in conjunction with integrated circuits, they cannot predict runtime (which is critical in mobile applications) and large- and small-signal steady-state and transient response performance over time of microscale FCs,

wherein fuel concentration decreases and fuel is exhausted with time and temperature and load are time dependent. The battery model proposed in [23] can potentially predict these parameters, but it has yet to be applied to FCs, which is the objective of the proposed model.

III. PROPOSED MICROSCALE FUEL CELL MODEL

The electrical behavior of microscale FCs, in other words, FCs with finite fuel capacity and changing concentrations, is modeled with interrelated runtime and current–voltage (I – V) subcircuit models, as shown in Fig. 2, which is derived, adapted from the lithium ion battery model proposed in [23], to which a nonlinear transient response feature is added. Runtime is modeled by loading a fixed-charge capacitor, dc behavior by a Thevenin-equivalent dependent voltage source, and asymmetrical transient response by R – C elements whose values for positive and negative transient events differ. Capacitor C_{Capacity} in the runtime subcircuit, therefore, represents the total fuel energy available in the system [state of charge (SoC)] and load-dependent current source I_{FC} and resistor R_{SD} model load current and methanol crossover (self-discharge) effects, both of which deplete this fuel energy. The I – V portion of the model emulates the open-circuit voltage of the FC with SoC-dependent voltage source V_{OC} , internal resistance with equivalent series resistor R_{Int} , and transient response performance with the RC network comprised of R_{Int} and nonlinear $C_{\text{Trans.eq}}$. From an electrical perspective, the proposed model should not only predict runtime, steady-state, and large- and small-signal transient response performance, but also be compatible with standard circuit simulators such as SPICE and SPICE-based cadence environments.

A. Usable Capacity

Usable energy or capacity nominally decreases with load current I_{FC} , the methanol crossover current induced by R_{SD} , and decreasing temperatures, but only if fuel pressure to the membrane and fuel concentration remain constant and no other interdependencies exist, which is not the case in microscale systems. When temperature increases, for instance, high methanol diffusion across the membrane causes an increase in methanol crossover current (i.e., leakage of unused methanol, which amounts to wasted energy), internal resistance R_{Int} decreases, and thanks to a strong reaction, open-circuit voltage V_{OC} increases. Usable capacity, as a result, is dependent on interrelated variables, whose interdependencies must be comprehended in the foregoing electrical model.

A tank completely filled with maximum concentration fuel corresponds to a fully precharged C_{Capacity} in the proposed model. The voltage across the capacitor for this condition is 1 V and is equivalent to an SoC of 100% (0 V or 0% SoC denotes a fully depleted tank). Capacitor voltage V_{SoC} consequently represents the methanol concentration of the DMFC, which is assumed to be uniform across the reservoir at any given time. This is a reasonable approximation for low to moderate discharge current conditions, before the DMFC enters the concentration polarization region, because the FC has the highest

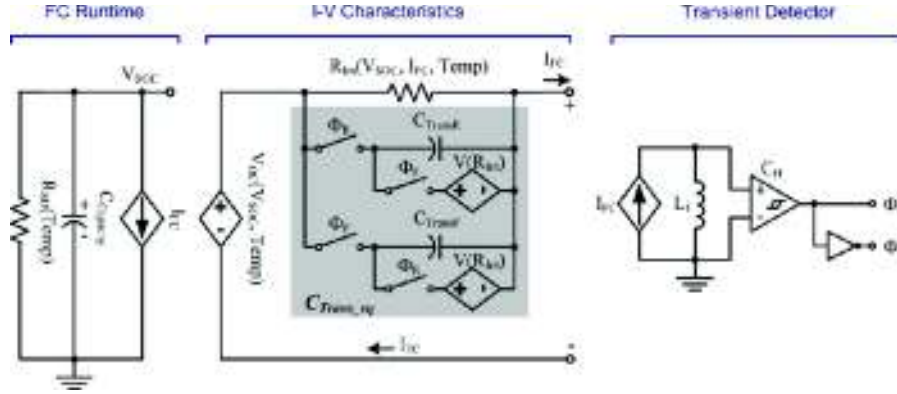


Fig. 2. Proposed cadence- and circuit-compatible microscale fuel cell model.

usable energy density when lightly loaded, and practical microsystems will condition the load for this effect.

Methanol crossover (leakage) is directly proportional to methanol concentration and increases with temperature [24]. The resistance of R_{SD} , therefore, represents methanol crossover effects and methanol concentration in the tank, having a net negative temperature coefficient (TC). Discharging $C_{Capacity}$ with load current I_{FC} and methanol leakage resistance R_{SD} effectively predicts the runtime performance of the system.

B. Open-Circuit Voltage

Open-circuit voltage V_{OC} depends on methanol concentration, or said differently, on SoC and temperature, which is why voltage-controlled voltage source V_{OC} is a function of V_{SoC} and temperature. High concentration, which implies higher methanol crossover, and therefore, larger voltage drops across the membrane, and/or low temperature conditions produce low open-circuit voltages [25]. The relationship between SoC and V_{OC} , in fact, is unique and independent of discharge current, as demonstrated from theory in [1] and [2] and experimentally later in this paper.

C. Polarization Curves

From an electrical perspective, the polarization curve reflects how the output voltage of an FC changes under various loading and concentration conditions. Internal resistor R_{Int} and voltage source V_{OC} embody these effects. Consequently, since these parameters are dependent on SoC, discharge current I_{FC} , temperature, and concentration, the performance of microscale FCs are described by a family of polarization curves, not just one curve, as experiments will show in later sections.

D. Transient Response

FCs respond slowly to changing loads because of their fuel-flow dependence and reaction kinetics. Maximum energy density performance is consequently achieved when FCs supply constant and continuous power, which is why capacitors, ultracapacitors, and/or batteries are used in conjunction with FCs to supply the changing portion of a given load. This is also why existing FC models only consider steady-state performance. A

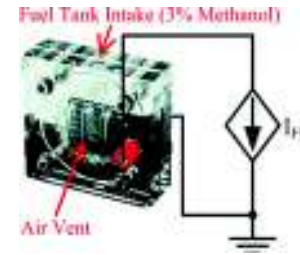


Fig. 3. DMFC prototype and its testing environment.

microscale system, however, does not have the luxury of bulky storage devices, and therefore, requires the transient response performance of an FC to be modeled.

Transient response is generally modeled with RC -dependent time constants and microscale FCs are no different, except FCs respond differently to rising and falling discharge currents, especially when fuel concentration (i.e., SoC) is low. Equivalent nonlinear capacitor C_{Tran_eq} captures these direction-dependent time constants. Comparator C_H detects whether the current is rising or falling and its output is used to control the connectivity of falling and rising capacitors C_{Tran_F} and C_{Tran_R} . For instance, when load current increases, the voltage across inductor L_1 increases, forcing Φ_F to disconnect C_{Tran_F} from the network and Φ_R to connect C_{Tran_R} into it (the opposite occurs when load current decreases). While one capacitor is connected, the other is precharged so that no voltage conflicts occur during transitions (i.e., voltages across C_{Tran_F} , C_{Tran_R} , and R_{Int} are always equal). The resulting RC response is first order for both directions. A higher order filter would be more accurate, but also complex.

IV. MODEL EXTRACTION AND MEASUREMENTS

Extracting all pertinent model parameters amount to subjecting several but similar FCs to a variety of discharge conditions. The prototypes used for this experiment were HydroGenius direct-methanol FC juniors from Heliocentris Energiesysteme GmbH (see Fig. 3) because fuel pressure is not regulated and the fuel tanks have finite fixed volumes. Fuel concentration consequently decreases with load and time, as any microscale FC would. The tank was filled with 3% methanol, which generates

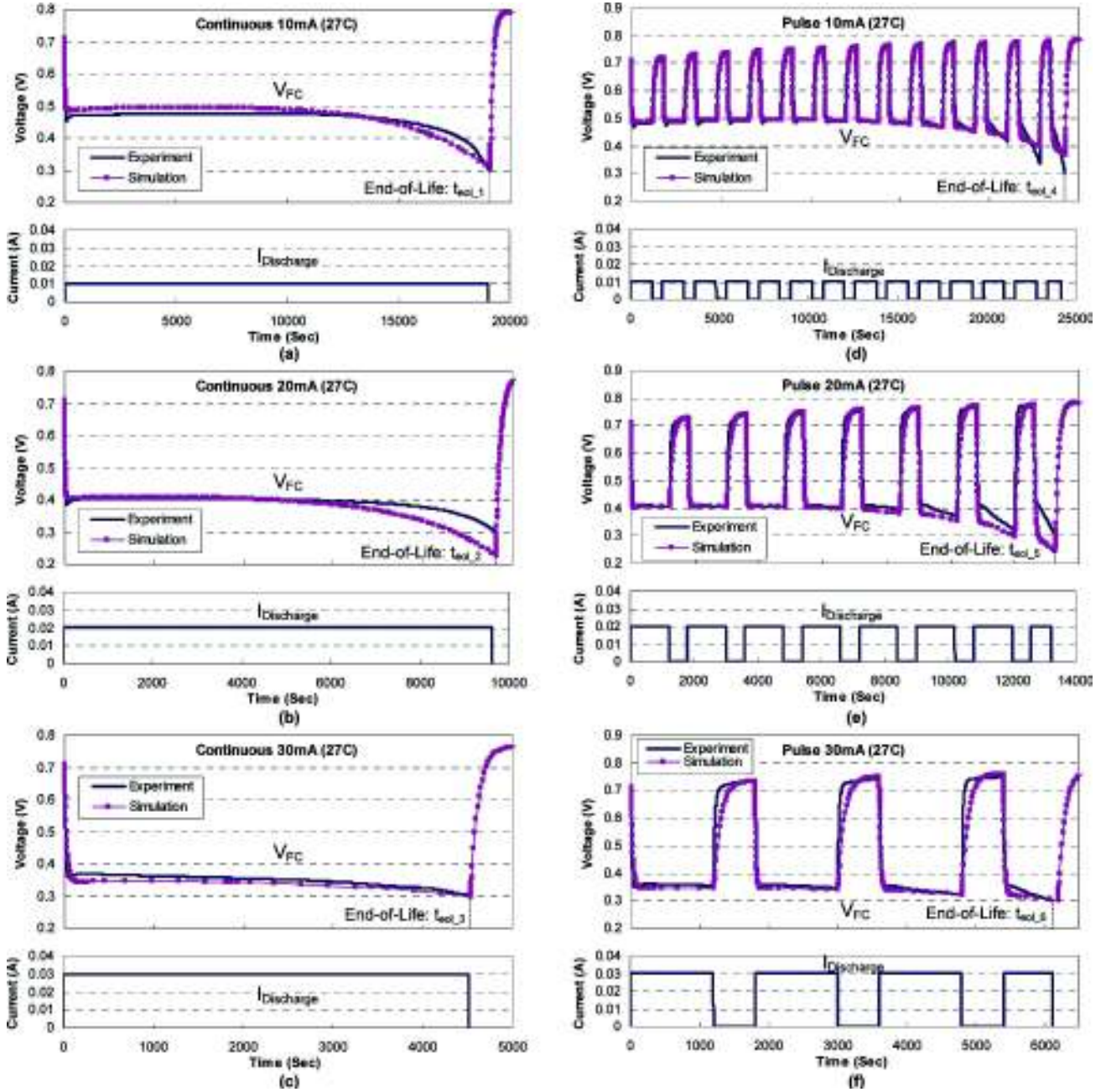


Fig. 4. Extracting (a)–(c) C_{Capacity} and self-discharge R_{SD} with three constant load currents and (d)–(f) open-circuit voltage V_{OC} , internal series resistor R_{Int} , and nonlinear transient response parameters C_{TranR} and C_{TranF} with three pulsed load profiles.

approximately 10 mW, and loaded with a user-defined load current at 27 °C. Since methanol crossover currents for these prototypes are on the same order of magnitude as the discharge currents, C_{Capacity} and R_{SD} cannot be measured directly, and that is why, a specially designed procedure is developed whereby no carbon dioxide (CO_2) analyzer, which is conventionally used to measure methanol crossover, is needed.

A. C_{Capacity} and R_{SD}

Continuous discharge currents I_1 , I_2 , and I_3 (10, 20, and 30 mA) were applied, as shown in Fig. 4(a)–(c), and run-

times $t_{\text{eol},1}$, $t_{\text{eol},2}$, and $t_{\text{eol},3}$ were subsequently measured at an end-of-life cell voltage of 300 mV. Assuming that SoC and fuel concentration are the same at a given end-of-life cell voltage, in other words, the energy remaining in the FC is the same at $t_{\text{eol},1}$, $t_{\text{eol},2}$, and $t_{\text{eol},3}$, results in a system of nonlinear equations from which C_{Capacity} and R_{SD} can be derived:

$$\begin{aligned} \text{SoC}|_{V_{\text{EOL}}} &\equiv V_{\text{SoC}}(I_1, t_{\text{eol},1}) \approx V_{\text{SoC}}(I_2, t_{\text{eol},2}) \\ &\approx V_{\text{SoC}}(I_3, t_{\text{eol},3}) \end{aligned} \quad (1)$$

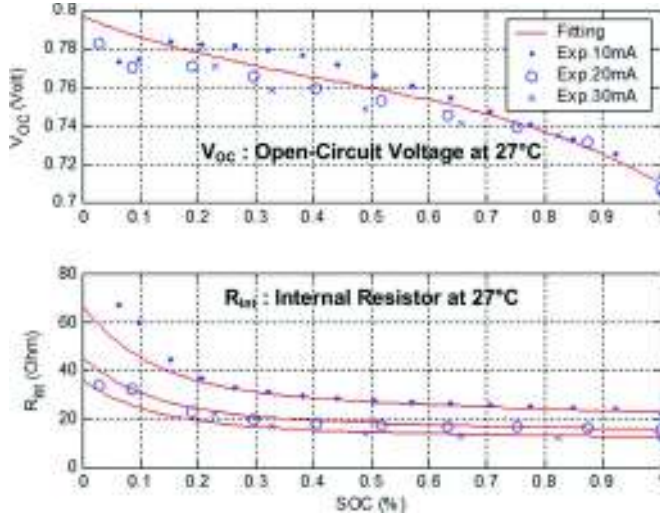


Fig. 5. Extracted and curve-fitted open-circuit voltage V_{OC} and internal resistance R_{Int} curves for increasing SoCs at 27 °C.

where V_{SoC} is

$$V_{SoC}(I_{FC}, t) = -I_{FC} R_{SD} + [V_{SoC}(0) + I_{FC} R_{SD}] e^{-t/R_{SD} C_{Capacity}} \quad (2)$$

and $V_{SoC}(0)$ is the initial voltage across $C_{Capacity}$ (i.e., initial SoC). In the foregoing model, because $C_{Capacity}$ is initialized to 1 V (i.e., SoC = 100% = 1), V_{SoC} is quantitatively equivalent to SoC, and therefore, used interchangeably.

B. V_{OC} , R_{Int} , and C_{Trans_eq}

The FC prototypes were subjected to three pulsed discharge currents: 0–10 mA (I_1), 20 mA (I_2), and 30 mA (I_3), as shown in Fig. 4(d)–(f), causing V_{SoC} (SoC) to decrease with time. Open-circuit voltages at decreasing values of SoC are therefore measured each time the load is in its 0 mA portion of the cycle, whereas internal series resistor R_{Int} is measured by dividing the unloaded-to-loaded voltage difference by the load current at the onset of each rising load step (see Fig. 5). Internal series resistor R_{Int} increases with decreasing SoC and decreases with increasing discharge current. As mentioned in Section III, open-circuit voltage V_{OC} increases with decreasing SoC, because lower concentration (i.e., low SoC) yields less methanol crossover, and therefore, a smaller voltage drop is lost across the membrane.

C_{TransR} and C_{TransF} set the rise- and fall-time responses of the FC to transient load-current events, and Fig. 4(d)–(f) indirectly shows how that response changes with time (with decreasing SoCs). First-order approximations were therefore extracted for each load step (i.e., decreasing SoCs) and shown in Fig. 6. The rising response is more consistent throughout the life of the FC, and slows down almost exponentially when the FC is close to fully drained, whereas the falling response slowly improves with decreasing SoCs. The resulting extracted model parameters and curve-fitted relationships are summarized in Table I.

TABLE I
EXTRACTED MODEL PARAMETERS AT 27 °C (V_{SoC} IS EQUIVALENT TO SoC)

$C_{Capacity} = 240F$	(3)
$R_{SD} = 268\Omega$	(4)
$V_{oc} = -0.1139 \cdot V_{SoC}^3 + 0.1463 \cdot V_{SoC}^2 - 0.1189 \cdot V_{SoC} + 0.7968$	(5)
$R_{Int} = (1.488e^{-4.226V_{SoC}} - 0.3066 \cdot V_{SoC} + 1.228) \cdot (-3.096E6 \cdot I_{FC}^3 + 2.082E5 \cdot I_{FC}^2 - 4869 \cdot I_{FC} + 55.53)$	(6)
$C_{TransR} = 1 + \left(\frac{1 - V_{SoC}}{0.85}\right)^{10}$	(7)
$C_{TransF} = 1 + V_{SoC}$	(8)

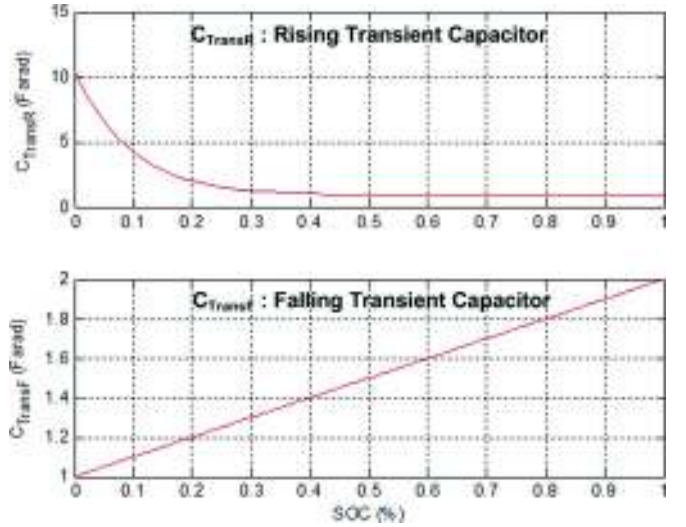


Fig. 6. Transient response parameter C_{TransR} and C_{TransF} dependence to SoC.

V. MODEL VALIDATION

The proposed model was simulated in cadence and used to predict the runtime and I - V performance of the FC. To validate the model and its ability to predict performance over the operational life of the FC, the prototype was subjected to four random load profiles and compared against their respective simulation results. The testing profiles were designed to embody various dissimilar duty-cycle and load-current combinations not included in the extraction procedure. The measurement results, which were conducted at room temperature, are illustrated in Fig. 7 and summarized in Table II. In all, less than 10.8% of runtime error and less than 72 mV of transient and steady-state error were observed for up to 95% of the operational life of the prototype, amounting to 14.1% mismatch error when normalized to its average voltage.

For conventional FC systems with constant fuel supply, the proposed model is still valid and relevant. In these cases, R_{SD} , $C_{Capacity}$, and I_{FC} , which constitute the SoC portion of the model, are not necessary, because SoC (i.e., fuel pressure and fuel concentration) remains unchanged and independent of load current. All other model parameters are therefore independent of V_{SoC} , yielding a model that is similar to the one presented in [21].

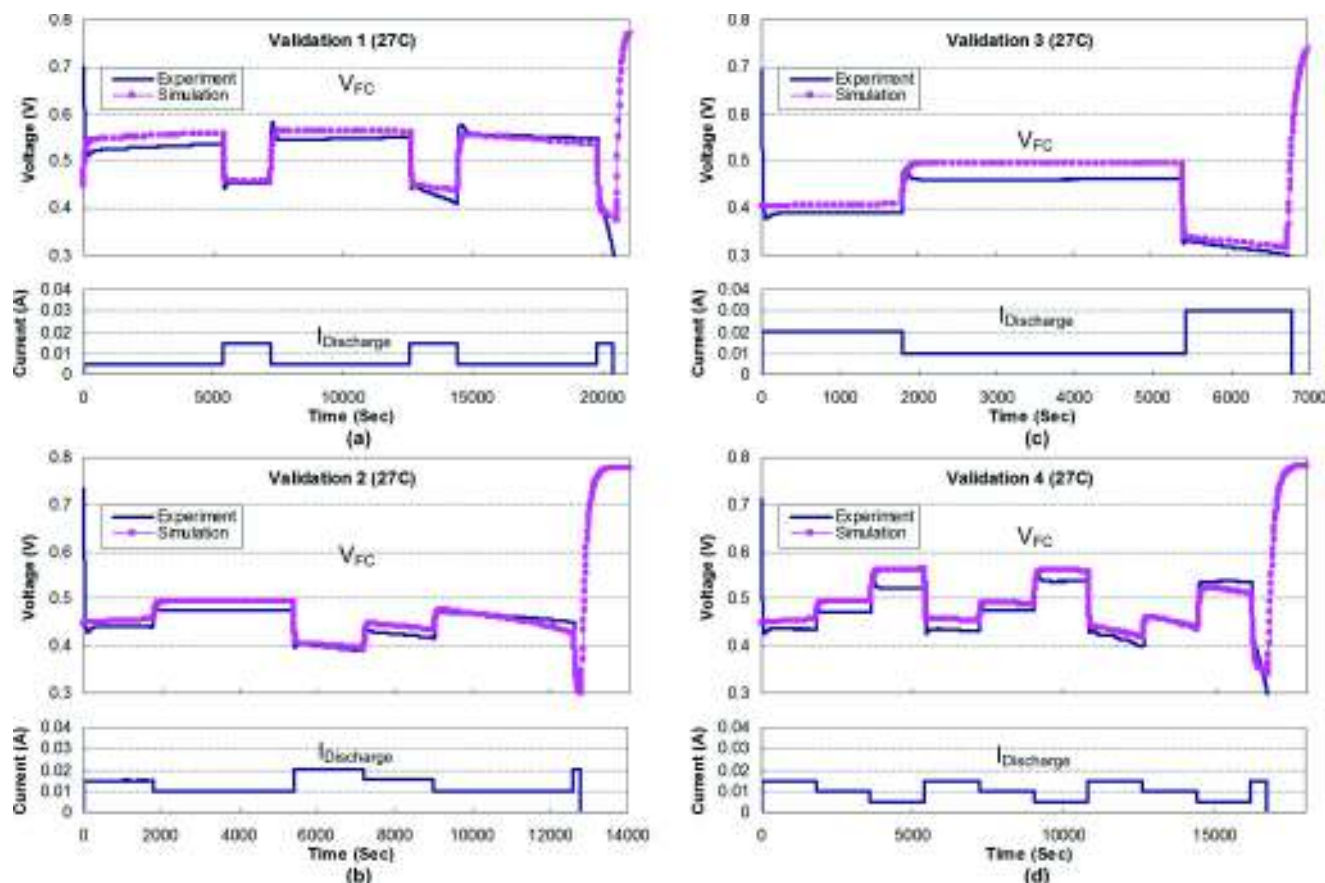


Fig. 7. Model validation through four random load profiles (a)–(d).

TABLE II
MODEL VALIDATION ACCURACY

Current Profiles	Avg.	Max. Error Voltage up to 95% Runtime (% of Avg.)	Runtime Error *
<i>From Extracted Data</i>			
10 mA cont.	460 mV	31 mV (6.7%)	0.9%
20 mA cont.	390 mV	70 mV (17.9%)	9.9%
30 mA cont.	350 mV	24 mV (6.9%)	0.4%
10 mA pulse	560 mV	67 mV (12.0%)	3.9%
20 mA pulse	510 mV	72 mV (14.1%)	10.8%
30 mA pulse	460 mV	32 mV (7.0%)	1.4%
<i>From Validation Data: Random Load Profiles</i>			
Validation 1	520 mV	36 mV (6.9%)	7.7%
Validation 2	450 mV	21 mV (4.7%)	0.1%
Validation 3	410 mV	35 mV (8.5%)	8.0%
Validation 4	470 mV	38 mV (8.1%)	4.1%
Worst-Case	510 mV	72 mV (14.1%)	10.8%
* Error = $[Runtime(Sim) - Runtime(Exp)] / Runtime(Exp)$			

VI. DISCUSSION

Errors during fast load-dump events result because the methanol concentration of the fuel across the tank changes with time and load variations; that is, to say, methanol diffusion rate at the side of the tank furthest away from the FC membrane does not track the near-side rate, which responds more readily to abrupt variations in current. This transient concentration gradi-

ent violates the uniform concentration assumption of the model. Further dissimilar time constants in the form of additional parallel RC network combinations can mitigate these errors, but they increase model complexity and complicate the extraction procedure, neither of which are appealing side effects. Microscale FC technology, however, is still relatively immature, and these improvements lose their effectiveness in the face of changing, inconsistent prototype performance (i.e., same experiments conducted at different times produce results with mismatches of up to 10 mV, as verified in Window B of Fig. 8).

The maturity of the technology is also a major cause of steady-state errors in the model. The voltage mismatch between Days 1 and 2 in Window C of Fig. 8, for instance, can be as much as 49 mV. After that, curve-fitting error is the next dominant error source. Higher order multivariable polynomials produce better results, but model and extraction complexity and additional simulation time obscure the benefits of marginal improvements, especially in light of the relative infancy of the technology. Curve-fitting functions matching average performance, although incapable of predicting exact performance, yield reasonable results. Yet another source of error is membrane aging, as shown in Window C of Fig. 8, where the voltage response of Day 91 is approximately 14 mV lower than that of Day 1. In the end, as SoC decreases and the FC reaches its end of life, technical maturity, curve fitting, and drift-over-time errors account for a steady-state error of up to 75 mV (Window D of Fig. 8) and runtime errors of up to 4.2% (end-of-life voltage variation).

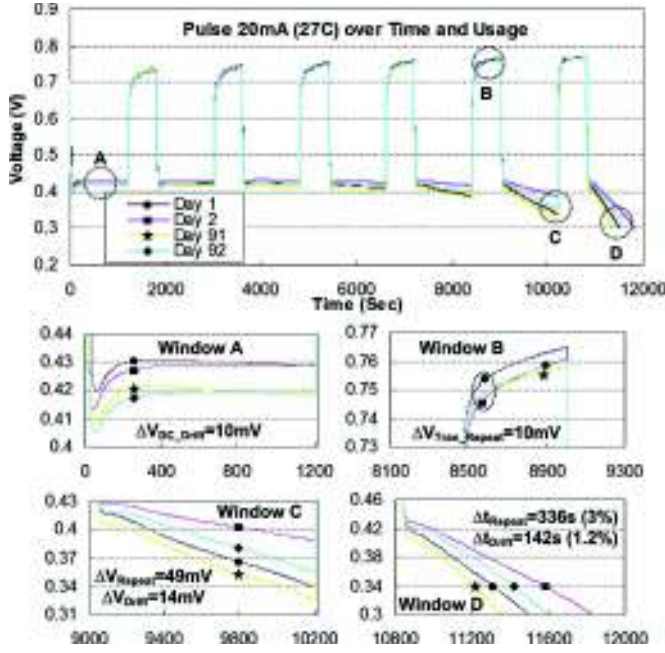


Fig. 8. Drift-over-time FC performance variations and various 1200 s zoomed-in windows.

However, as has been the case for batteries, the consistency and uniformity of microscale FCs, as well as voltage and runtime errors in the model, are expected to improve with time, as the technology matures.

VII. TEMPERATURE EFFECTS

Almost every parameter in the proposed model is dependant on temperature. Unlike many macroscale solutions, however, the intrinsic (internal) temperature of the microscale FC is approximately equal to its extrinsic (external) value because the power levels are low, on the order of 3–10 mW/cm². Therefore, considering the relatively low thermal impedance of the heat-sinking liquid methanol–metal electrode medium, which can be 10–60 °C/W, the FC’s temperature is almost entirely set (to within 1 °C–2 °C) by the environment in which it sits, not the power it delivers. Complicating the model to address this small variation has little effect on overall accuracy, but considerable adverse effects on computational time and extraction complexity. Therefore, to evaluate temperature effects and circumvent, the drift-over-time issues discussed in the previous section, model parameters for newly acquired FC prototypes were extracted at various extrinsic temperatures (27 °C, 40 °C, and 50 °C) and shown and listed in Fig. 9 and Tables III and IV.

Self-discharge R_{SD} (see Table III) and internal resistor R_{Int} (see Fig. 9) decrease with temperature, because methanol crossover leakage current and FC conductivity both increase with temperature. Near the FC’s end of life, however, when SoC is below 10%, R_{Int} ’s trend reverses, and this is mostly the result of resolution limits in the experiments, i.e., limited data for the high $dR_{Int}/dSoC$ slope present. Open-circuit voltage V_{OC} (see Fig. 9) increases with temperature because the reaction rate increases, but model parameter $C_{Capacity}$ remains

TABLE III
EXTRACTED MODEL PARAMETERS AT 27 °C, 40 °C, AND 50 °C (V_{SoC} IS QUANTITATIVELY EQUIVALENT TO SoC)

MODEL PARAMETERS	27 °C	40 °C	50 °C
$C_{Capacity}$ (F)	239	244	240
R_{SD} (Ω)	109	95.5	61.5
V_{OC} (V)			
$V_{OC}(27^{\circ}C) = -0.09317 \cdot V_{SoC}^3 + 0.127 \cdot V_{SoC}^2 - 0.1044 \cdot V_{SoC} + 0.7859$ (9)			
$V_{OC}(40^{\circ}C) = -0.1833 \cdot V_{SoC}^3 + 0.2844 \cdot V_{SoC}^2 - 0.1967 \cdot V_{SoC} + 0.8124$ (10)			
$V_{OC}(50^{\circ}C) = -0.2815 \cdot V_{SoC}^3 + 0.5199 \cdot V_{SoC}^2 - 0.3546 \cdot V_{SoC} + 0.8649$ (11)			
R_{Int} (Ω)			
$R_{Int}(27^{\circ}C) = (0.9142e^{-5.358V_{SoC}} - 0.3012 \cdot V_{SoC} + 1.309) \cdot (-1.46E6 \cdot I_{FC}^3 + 1.089E5 \cdot I_{FC}^2 - 2984 \cdot I_{FC} + 42.38)$ (12)			
$R_{Int}(40^{\circ}C) = (1.384e^{-9.333V_{SoC}} - 0.2409 \cdot V_{SoC} + 1.194) \cdot (-1.417E6 \cdot I_{FC}^3 + 1.069E5 \cdot I_{FC}^2 - 2934 \cdot I_{FC} + 40.17)$ (13)			
$R_{Int}(50^{\circ}C) = (2.612e^{-13.02V_{SoC}} - 0.2441 \cdot V_{SoC} + 1.18) \cdot (-7.795E5 \cdot I_{FC}^3 + 6.697E4 \cdot I_{FC}^2 - 2134 \cdot I_{FC} + 34.09)$ (14)			
$C_{Transit}$ (F)			
$C_{Transit} = 1 + \left(\frac{1 - V_{SoC}}{0.85} \right)^{10}$ (15)			
$C_{Transit} = 1 + V_{SoC}$ (16)			

TABLE IV
MODEL EXTRACTION ACCURACY OVER TEMPERATURE

Current Profiles		Avg.	Max. Error Voltage up to 95% Runtime (% of Avg.)	Runtime Error *
27 °C	10 mA cont.	490 mV	25 mV (5.1%)	8.4%
	20 mA cont.	420 mV	49 mV (11.7%)	9.5%
	30 mA cont.	360 mV	23 mV (6.4%)	7.3%
	10 mA pulse	520 mV	52 mV (10.0%)	7.8%
	20 mA pulse	510 mV	36 mV (7.1%)	3.2%
	30 mA pulse	470 mV	37 mV (7.9%)	8.5%
40 °C	10 mA cont.	490 mV	31 mV (6.3%)	4.6%
	20 mA cont.	440 mV	49 mV (11.1%)	4.2%
	30 mA cont.	410 mV	71 mV (17.3%)	10.5%
	10 mA pulse	550 mV	35 mV (6.4%)	4.5%
	20 mA pulse	550 mV	41 mV (7.5%)	2.5%
	30 mA pulse	530 mV	41 mV (7.7%)	0.4%
50 °C	10 mA cont.	570 mV	69 mV (12.1%)	0.3%
	20 mA cont.	510 mV	80 mV (15.7%)	6.8%
	30 mA cont.	470 mV	36 mV (7.7%)	8.8%
	10 mA pulse	600 mV	79 mV (13.2%)	4.1%
	20 mA pulse	590 mV	37 mV (6.3%)	1.6%
	30 mA pulse	570 mV	69 mV (12.1%)	0.3%
Worst-Case		510 mV	80 mV (15.7%)	10.5%
* Error = $ [Runtime(Sim) - Runtime(Exp)] / Runtime(Exp) $				

relatively constant across temperature because energy is conserved. In all, less than 10.5% of runtime error and less than 80 mV (15.7%) of voltage error were observed.

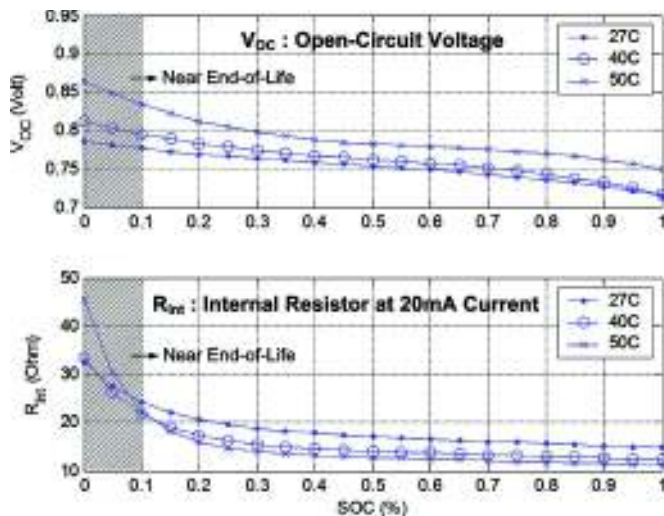


Fig. 9. Extracted open-circuit voltage V_{OC} and internal resistance R_{Int} values for increasing SoCs at 27 °C, 40 °C, and 50 °C.

VIII. CONCLUSION

A compact microscale electrical FC model capable of predicting steady-state and transient response performance with better than 80 mV (15.7%) accuracy over 95% of its operational life and predicting runtime within 10.8% has been presented and experimentally validated, in spite of the variability of relatively immature state-of-the-art FC technologies. The model is fully cadence compatible, which is an industry standard platform for simulating and designing integrated circuits, and capable of capturing the finite tank capacities and changing fuel concentrations prevalent in microscale systems, while still catering to the current- and temperature-dependant capacities, nonlinear open-circuit voltages, methanol crossover currents, internal resistances, and slow kinetics of conventional macroscale FCs. Given the growing demands of portable handheld electronics and their consequential drive toward system-in-package (SiP) dimensions, microscale FCs are becoming attractive solutions, and predicting their performance over the runtime of the system is crucial in meeting the increasingly stringent performance requirements of wireless mixed-signal systems. The proposed model is therefore an enabling mechanism through which today's research in microscale FCs can be bridged to tomorrow's SiP solutions.

REFERENCES

- [1] EG&G Technical Services, Inc., and Science Applications International Corporation, *Fuel Cell Handbook*, 6th ed., Morgantown, VA: U.S. Department of Energy, Office of Fossil Energy, National Energy Technology Laboratory, 2002, ch. 1.
- [2] G. Hoogers, *Fuel Cell Technology Handbook*. Boca Raton, FL: CRC, 2003, ch. 1.
- [3] C. K. Dyer, "Fuel cells for portable applications," *J. Power Sources*, vol. 106, no. 1–2, pp. 31–34, Apr. 2002.
- [4] C. Hebling and U. Groos, "Miniature fuel cell systems for consumer applications," in *Proc. Fuel Cell World*, Lucerne, Switzerland, Jul. 2002, pp. 41–48.
- [5] T. L. Macdonald, "Fuel cells for portable devices: Weak link or ideal power source?," *EDN Power Suppl.*, pp. 31–34, Sep. 2002.
- [6] W. Y. Sim, G. Y. Kim, and S. S. Yang, "Fabrication of micro power source (MPS) using a micro direct methanol fuel cell (μ DMFC) for the medical

- application," in *Proc. 14th IEEE Int. Conf. Micro Electro Mech. Syst.*, Interlaken, Switzerland, 2001, pp. 341–344.
- [7] K. Min, S. Tanaka, and M. Esashi, "Silicon-based micro-polymer electrolyte fuel cells," in *Proc. 16th IEEE Int. Conf. Micro Electro Mech. Syst.*, Jan. 2003, pp. 379–382.
- [8] T. J. Yen, N. Fang, X. Zhang, G. Q. Lu, and C. Y. Wang, "A micro methanol fuel cell operating at near room temperature," *Appl. Phys. Lett.*, vol. 83, no. 19, pp. 4056–4058, Nov. 2003.
- [9] C. W. Moore, J. Li, and P. A. Kohl, "Microfabricated fuel cells with thin-film silicon dioxide proton exchange membranes," *J. Electrochem. Soc.*, vol. 152, no. 8, pp. A1606–A1612, Aug. 2005.
- [10] R. F. Savinell, J. S. Wainright, L. Dudik, and C. C. Liu, "Recent advances in microfabricated fuel cells," in *New Mater. Electrochem. Syst.*, Montreal, QC, Canada, Jul. 2001, pp. 371–372.
- [11] D. Strassberg, "The glass is half full... with methanol fuel," *Electron. Design Netw. (EDN)*, May 2004, pp. 53–60.
- [12] H. L. Maynard and J. P. Meyers, "Miniature fuel cells for portable power: Design considerations and challenges," *J. Vacuum Sci. Technol. B (Microelectron. Nanometer. Struct.)*, vol. 20, no. 4, pp. 1287–1297, Jul. 2002.
- [13] R. F. Mann, J. C. Amphlett, M. A. I. Hooper, H. M. Jensen, B. A. Peppley, and P. R. Roberge, "Development and application of a generalized steady-state electrochemical model for a PEM fuel cell," *J. Power Sources*, vol. 86, pp. 173–180, Mar. 2000.
- [14] L. Y. Chiu, B. Diong, and R. S. Gemmen, "An improved small-signal model of the dynamic behavior of PEM fuel cells," *IEEE Trans. Ind. Appl.*, vol. 40, no. 4, pp. 970–977, Jul.–Aug. 2004.
- [15] W. Friede, S. Rael, and B. Davat, "Mathematical model and characterization of the transient behavior of a PEM fuel cell," *IEEE Trans. Power Electron.*, vol. 19, no. 5, pp. 1234–1241, Sep. 2004.
- [16] P. Argyropoulos, K. Scott, A. K. Shukla, and C. Jackson, "A semi-empirical model of the direct methanol fuel cell performance. I. Model development and verification," *J. Power Sources*, vol. 123, pp. 190–199, Sep. 2003.
- [17] S. Yerramalla, A. Davari, A. Feliachi, and T. Biswas, "Modeling and simulation of the dynamic behavior of a polymer electrolyte membrane fuel cell," *J. Power Sources*, vol. 124, pp. 104–113, Oct. 2003.
- [18] K. Sedghisigarchi and A. Feliachi, "Dynamic and transient analysis of power distribution systems with fuel cells—Part I: Fuel-cell dynamic model," *IEEE Trans. Energy Convers.*, vol. 19, no. 2, pp. 423–428, Jun. 2004.
- [19] J. M. Correa, F. A. Farret, L. N. Canha, and M. G. Simoes, "An electrochemical-based fuel-cell model suitable for electrical engineering automation approach," *IEEE Trans. Ind. Electron.*, vol. 51, no. 5, pp. 1103–1112, Oct. 2004.
- [20] D. Yu and S. Yuvarajan, "A novel circuit model for PEM fuel cells," in *Proc. 2004 IEEE Appl. Power Electron. Conf. Expo.*, vol. 1, pp. 362–366.
- [21] P. Famouri and R. S. Gemmen, "Electrochemical circuit model of a PEM fuel cell," in *Proc. 2003 IEEE Power Eng. Soc. Gen. Meet.*, Jul., vol. 3, pp. 1436–1440.
- [22] J. Garnier, M. C. Pera, D. Hissel, F. Harel, D. Candusso, N. Glandut, J. P. Diard, A. D. Bernardinis, J. M. Kauffmann, and G. Coquery, "Dynamic PEM fuel cell modeling for automotive applications," in *Proc. 2003 IEEE 58th Veh. Technol. Conf.*, Oct. vol. 5, pp. 3284–3288.
- [23] M. Chen and G. A. Rincón-Mora, "An accurate electrical battery model capable of predicting runtime and I–V performance," *IEEE Trans. Energy Convers.*, vol. 21, no. 2, pp. 504–511, Jun. 2006.
- [24] S. R. Narayanan, A. Kindler, B. Jeffries-Nakamura, W. Chun, H. Frank, M. Smart, T. I. Valdez, S. Surampudi, and G. Halpert, "Recent advances in PEM liquid-feed direct methanol fuel cells," in *Proc. 1996 11th Battery Conf. Appl. Adv.*, Long Beach, CA, Jan., pp. 113–122.
- [25] Z. Qi and A. Kaufman, "Open circuit voltage and methanol crossover in DMFCs," *J. Power Sources*, vol. 110, pp. 177–185, Jul. 2002.



Min Chen (S'04) was born in Jingdezhen, China. He received the B.Eng. degree (with highest honors) and the M.Eng. degree in electrical engineering from the Southeast University, Nanjing, China, in 1999 and 2002, respectively. He is currently working toward the Ph.D. degree in electrical and computer engineering at the Georgia Institute of Technology, Atlanta.

His current research interests include analog and power IC design, more specifically, battery and fuel cell modeling, high efficiency charger IC design, and integrated power management for hybrid power sources.



Gabriel A. Rincón-Mora (S'91–M'97–SM'01) received the B.S.E.E. degree (high honors) in electrical engineering from Florida International University, University Park, in 1992, and the M.S.E.E. and Ph.D. (outstanding Ph.D. graduate) degrees in electrical engineering from Georgia Tech, Atlanta, in 1994 and 1996, respectively.

From 1994 to 2003, he was with Texas Instruments as a Senior Integrated Circuits Designer, Design Team Leader, Member of Group Technical Staff, and Analog Consultant, where he has engaged in re-

search on integrated power management circuits for products such as cellular phones, pagers, laptop, and desktop computers. During 1999, he was appointed Adjunct Professor for Georgia Tech, where he later became a Full Time Faculty Member of the School of Electrical and Computer Engineering. During 2002–2004, he was the Director of the Georgia Tech Analog Consortium. He has designed and released over 26 power management IC products. He also teaches short courses on analog and power management IC design. He holds 25 patents. He is the author or coauthor of more than 84 publications, two of which are books titled *Voltage References* and *Power Management ICs*.

Dr. Rincón-Mora was the Vice-Chairman for the joint Atlanta IEEE Solid-State Circuits Society and Circuits and Systems (SSCS–CAS) Chapter for 2004, and has been its Chairman since 2005. He is the recipient of the National Hispanic in Technology Award from the Society of Professional Hispanic Engineers, the Charles E. Perry Visionary Award from Florida International University, and a Commendation Certificate from the Lieutenant Governor of California for his work and contributions to the field. He was inducted into the Council of Outstanding Young Engineering Alumni by Georgia Tech and featured on the cover of *Hispanic Business Magazine* as one of The 100 Most Influential Hispanics, *La Fuente*, and three times on *Nuevo Impacto*.